

Supporting Information

Cationic Zr catalysts for the Sequential Polymerisation of Alkenes and Cyclic Oxygenated Monomers

Eszter Fazekas^a, Carole A. Morrison^a, Jennifer A. Garden^a

^a EaStCHEM School of Chemistry, The University of Edinburgh, UK

Email address: j.garden@ed.ac.uk

Table of contents

General experimental considerations	1
Synthesis of amine bis(phenolate) ligand ABPH₂	3
Synthesis of ABPZr(Bn)₂	3
<i>In situ</i> generation of cationic species	3
General procedure for homopolymerisations	4
General procedure for sequential polymerisations.....	4
Polymerisation data.....	5
NMR spectra of polymerisation product mixtures	5
MALDI-ToF spectra of obtained polymers.....	9
SEC chromatograms of obtained polymers	10
DFT calculations.....	12
References.....	14

General experimental considerations

All manipulations requiring inert conditions were performed under an argon atmosphere using standard Schlenk techniques or a glovebox. The amine bisphenolate ligand (**ABPH₂**) and the corresponding Zr complex (**ABPZrBn₂**) were synthesised *via* previously reported procedures.^{1,}
² Reagents and solvents were obtained from STREM, TCI Chemicals, Merck or Acros and were used without further purification unless described otherwise. Dry solvents were collected from a solvent purification system (Innovative Technologies), and stored over activated 4 Å molecular sieves under an argon atmosphere. Benzene-*d*₆ and toluene-*d*₈ were dried over

CaH₂, distilled under argon and stored over activated 4 Å molecular sieves in a glovebox. 1-Hexene, styrene, methyl methacrylate, isoprene and myrcene were dried over CaH₂, vacuum-transferred into an ampoule and stored in a glovebox at -34 °C. ε-Caprolactone (ε-CL), β-butyrolactone (β-BL), propylene oxide (PO), cyclohexene oxide (CHO) and limonene oxide (LO) were dried over CaH₂ purified by (vacuum) distillation and stored in the glovebox at -34 °C. *rac*-Lactide was recrystallised from toluene and sublimed twice. ¹H and ¹³C spectra were recorded on Bruker AVA500 or AVA600 spectrometers at 298 K at 500 MHz or 600 MHz and referenced to the residual solvent peaks (¹H: δ 7.16 (C₆D₆), δ 7.26 (CDCl₃)). ¹¹B and ¹⁹F NMR spectra were recorded on AVA400 or PRO500 spectrometers. Diffusion-Ordered Spectroscopy (DOSY) NMR experiments were performed at 298 K on a Bruker Ascend 2 channel instrument operating at a frequency of 500 MHz for proton resonance under TopSpin (version 4.1.3, Bruker Biospin, Karlsruhe) and equipped with a z-gradient DCH/5mm tuneable "CryoProbe"™ probe and a GRASP II gradient spectroscopy accessory providing a maximum gradient output of 53.5 G/cm (5.35G/cmA). Diffusion ordered NMR data was acquired using the Bruker pulse program *dstebpgp3s* with a spectral width of 10330 Hz (centred on 6.175 ppm) and 32768 data points. A relaxation delay of 2 s was employed along with a diffusion time (Δ) of 100 ms and a longitudinal eddy current delay (LED) of 5 ms. Bipolar gradient pulses (δ/2) of 1.5 ms and homospoil gradient pulses of 0.6 ms were used. The gradient strengths of the 3 homospoil pulses were -13.17%, -17.13%, -15.37%. 16 experiments were collected with the bipolar gradient strength, initially at 5% (1st experiment), linearly increased to 95% (16th experiment). All gradient pulses were smooth-square shaped (SMSQ10.100) and after each application a recovery delay of 200 μs used. The experiment was run with 16 scans per increment, employing one stimulated echo with two spoiling gradients. All NMR spectroscopic analysis were performed with MestReNova, Version 14. SEC analyses of polymer samples were carried out in GPC grade THF at a flow rate of 1 mL min⁻¹ at 35 °C on an Agilent 1260 Infinity II GPC/SEC single detection system with mixed bed C PLgel columns (300 x 7.5 mm) and a refractive index detector. MALDI-ToF MS analyses were performed using a Bruker Daltonics UltrafleXtreme™ MALDI-ToF/ToF MS instrument in either linear or reflectron mode. MALDI-ToF samples were made up in a volume ratio of *a*) 2:2:1 of polymer (10 mg/mL), dithranol (10 mg/mL) and KI (ionising agent, 10 mg/mL) in THF. A droplet (2 μL) of the resultant mixture was spotted on to the sample plate. All analysis were performed with Bruker Compass DataAnalysis, Version 5.0 SR1.

General procedure for homopolymerisations

In a glovebox, a vial equipped with magnetic stirrer and PTFE-lined cap was charged with 0.0125 mmol pre-catalyst (9.95 mg of **ABPZrBn₂** or 3.14 mg of **Cp₂ZrMe₂**), 1 equiv. of co-catalyst [0.0125 mmol, 6.40 mg of tris(pentafluorophenyl)borane or 11.52 mg of trityl tetrakis(pentafluorophenyl)borate] and an appropriate volume of toluene to achieve 1 M final monomer concentration. The mixture was stirred at room temperature for 10 minutes to form the catalytically active cationic species. Subsequently, 50-100 equiv. monomer (1-hexene, styrene, isoprene, myrcene, propylene oxide, cyclohexene oxide, limonene oxide, ϵ -caprolactone, β -butyrolactone or *rac*-lactide) was added with an automatic pipette, and the mixture was stirred at the appropriate reaction temperature for the specified reaction time. The polymerisation vial was removed from the glovebox, the polymerisation quenched with CDCl₃ (approximately 1 mL), and then an aliquot of the crude mixture was analysed *via* ¹H NMR spectroscopy to determine the monomer conversion. The remainder of the reaction mixture was purified by precipitation in acidified methanol (MeOH/HCl(aq), approximately 75:1 mL). The polymer was isolated by filtration and was subsequently dried *in vacuo* until constant weight was achieved. Samples for SEC analysis were prepared in HPLC grade THF and filtered through a 0.2 μ m pore-sized PTFE syringe filter.

General procedure for sequential polymerisations

In a glovebox, a vial equipped with magnetic stirrer and PTFE-lined cap was charged with 0.0125 mmol pre-catalyst (9.95 mg of **ABPZrBn₂** or 3.14 mg of **Cp₂ZrMe₂**), 1 equiv. of co-catalyst [0.0125 mmol, 6.40 mg of tris(pentafluorophenyl)borane or 11.52 mg of trityl tetrakis(pentafluorophenyl)borate] and an appropriate volume of toluene to achieve 1 M final monomer concentration. The mixture was stirred at room temperature for 10 minutes to form the catalytically active cationic species. After this, 50-100 equiv. of the first monomer (typically 1-hexene) was added with an automatic pipette, and the mixture was stirred at room temperature for 10 minutes or until the first monomer was fully consumed (conversion was determined through ¹H NMR analysis of aliquots taken with a syringe). The second monomer (ϵ -CL or PO) was sequentially added and the mixture was stirred at the appropriate reaction temperature for the specified reaction time. The reaction vial was then removed from the glovebox, the polymerisation quenched with CDCl₃ (approximately 1 mL), and then an aliquot of the crude reaction mixture was analysed *via* ¹H NMR spectroscopy to determine the monomer conversion. The remainder of the reaction mixture was purified by precipitation in acidified methanol (MeOH/HCl(aq), approximately 75:1 mL), washed with hot hexane (and in some cases further purified *via* Soxhlet extraction). The polymer was isolated by filtration and was subsequently dried *in vacuo* until constant

weight was achieved. Samples for SEC analysis were prepared in HPLC grade THF and filtered through a 0.2 μm pore-sized PTFE syringe filter.

Polymerisation data

Table S1: Additional homopolymerisation data.

Entry	Monomer	Pre-cat.	Co-cat.	Monom. equiv.	T (°C)	t (h)	Conv. (%)	$M_{n,th}$ (kg/mol)	$M_{n,SEC}$ (kg/mol)	\bar{D}
1	1-hexene	ABPZrBn ₂	BCF	50	r.t.	0.33	>99	4.2	11	1.9
2	1-hexene	ABPZrBn ₂	-	100	r.t.	24	0	-	-	-
3	1-hexene	-	BCF	100	r.t.	24	0	-	-	-
4	isoprene	Cp ₂ ZrMe ₂	BCF	50	75	18	0	-	-	-
5	isoprene	Cp ₂ ZrMe ₂	TBCF	50	75	20	>99	3.4	< 1	-
6	myrcene	Cp ₂ ZrMe ₂	BCF	50	75	48	0	-	-	-
7	myrcene	Cp ₂ ZrMe ₂	TBCF	50	75	20	45	3.1	< 1	-
8	ϵ -CL	ABPZrBn ₂	BCF	100	r.t.	4	78	8.9	15.9	1.12
9	ϵ -CL	ABPZrBn ₂	BCF	100	r.t.	24	>99	11.4	17.25	1.21
10	ϵ -CL	ABPZrBn ₂	TBCF	100	r.t.	4	76	8.7	15.4	1.09
11	ϵ -CL	ABPZrBn ₂	TBCF	100	r.t.	24	>99	11.4	18.8	1.15
12	ϵ -CL	ABPZrBn ₂	-	100	75	2	21	2.4	25.7	1.96
13	ϵ -CL	-	BCF	100	75	2	0	-	-	-
14	ϵ -CL	Cp ₂ ZrMe ₂	BCF	100	r.t.	4	95	10.8	3.6	2.04
15	<i>rac</i> -LA	ABPZrBn ₂	BCF	50	120	20	44	3.2	3.3, 0.6	1.2, 1.3
16	β -BL	ABPZrBn ₂	BCF	100	75	2	63	5.4	< 1.0	-
17	PO	ABPZrBn ₂	-	100	r.t.	24	0	-	-	-
18	PO	Cp ₂ ZrMe ₂	BCF	100	r.t.	0.33	>99	5.8	< 1.0	-
19	PO	-	BCF	100	r.t.	5 min	>99	5.8	< 1.0	-
20	PO	-	TBCF	100	r.t.	5 min	>99	5.8	< 1.0	-
21	CHO	ABPZrBn ₂	BCF	50	r.t.	0.33	>99	4.9	< 1.0	-
22	LO	ABPZrBn ₂	BCF	50	r.t.	1	>99	7.6	1.2	1.3

Conditions: 0.0125 mmol of ABPZrBn₂ or Cp₂ZrMe₂ and BCF or TBCF pre-stirred in toluene for 10 minutes prior to the addition of monomer to afford 1M concentration of monomer in toluene. SEC – uncorrected values against polystyrene standards, except for PCL samples, which were corrected with a correction factor of 0.56.

NMR spectra of polymerisation product mixtures

The ¹H NMR spectra of crude product mixtures from the homopolymerisation of isoprene, myrcene, styrene, cyclohexene oxide, limonene oxide, β -butyrolactone and *rac*-lactide were analysed and compared to literature.³⁻⁸

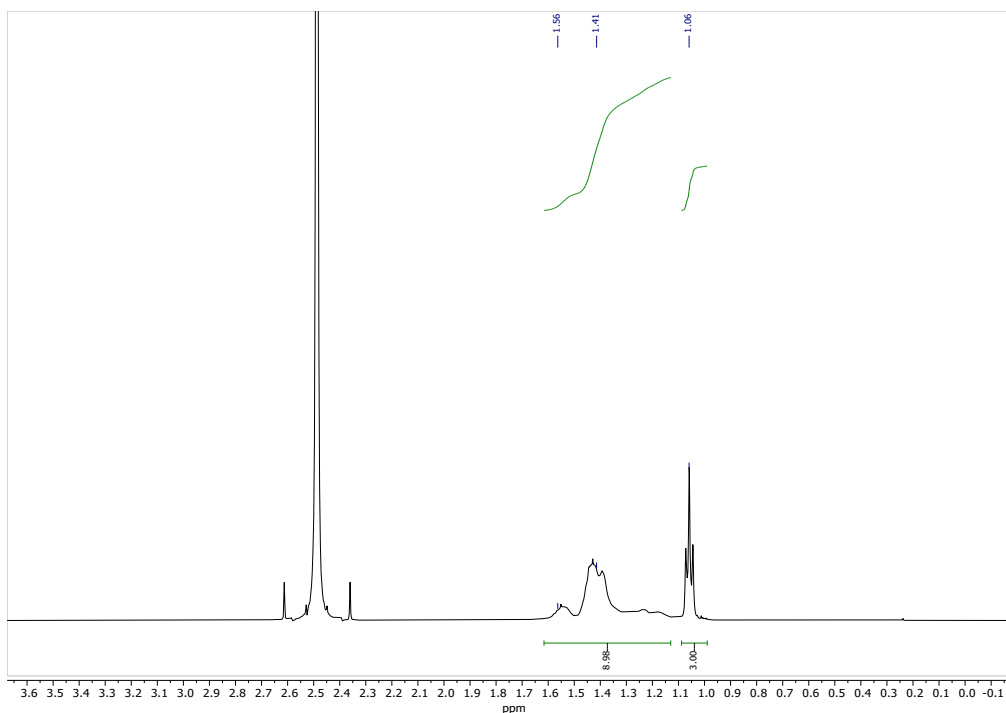


Figure S4: Representative crude ^1H NMR spectrum of a 1-hexene polymerisation using catalyst $1/\text{BnB}(\text{C}_6\text{F}_5)_3^-$, analysed in CDCl_3 at 20°C . Conversion was determined via integration of the triplet polymer peak at 1.06 ppm against the corresponding 1-hexene (monomer) peak at 0.93 ppm.

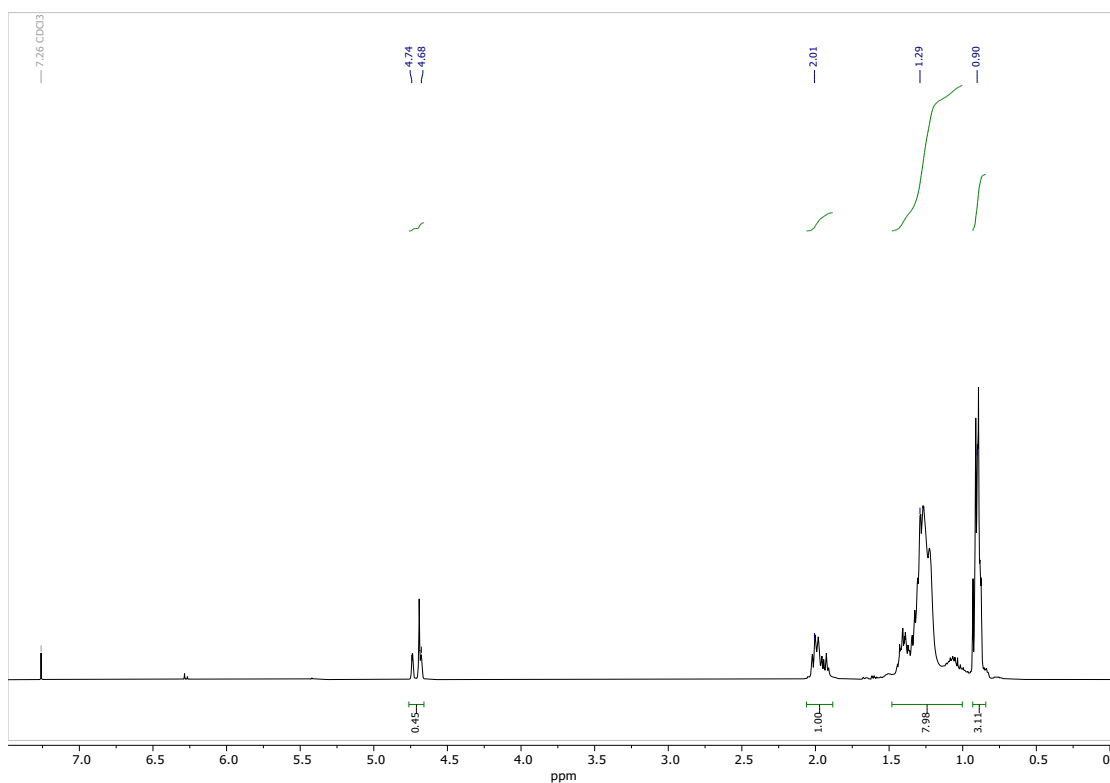


Figure S5: Representative crude ^1H NMR spectrum of a 1-hexene polymerisation using catalyst $2/\text{MeB}(\text{C}_6\text{F}_5)_3^-$ affording olefin-capped PH as indicated by vinylene and vinylidene resonances (4.68 and 4.74 ppm), analysed in CDCl_3 at 20°C .

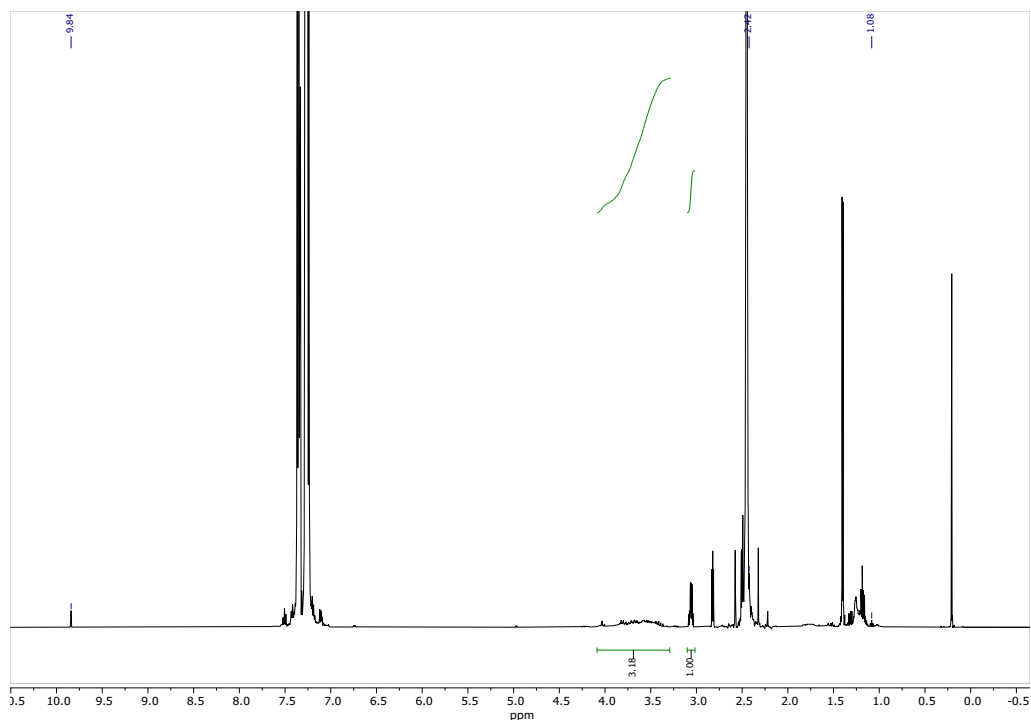


Figure S6: Representative crude ^1H NMR spectrum of a propylene oxide polymerisation showing the characteristic aldehyde resonance at 9.84 ppm for the propionaldehyde side product, analysed in CDCl_3 at 20°C . Quantitative conversion was signalled by the complete disappearance of propylene oxide monomer CH and CH_2 peaks (2.32, 2.64 and 2.88 ppm).

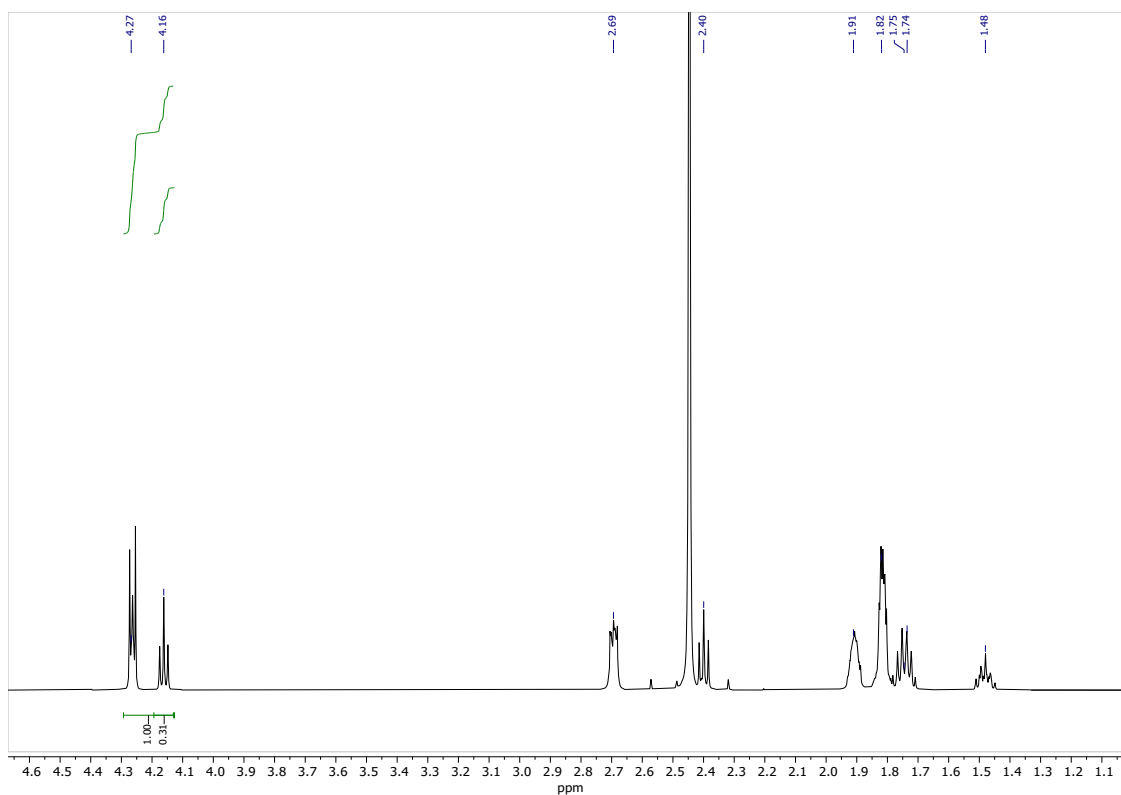


Figure S7: Representative crude ^1H NMR spectrum of $\epsilon\text{-CL}$ polymerisation, analysed in CDCl_3 at 20°C , and showing the monomer peak (4.27 ppm) and polymer peak (4.16 ppm) used for calculating conversion.

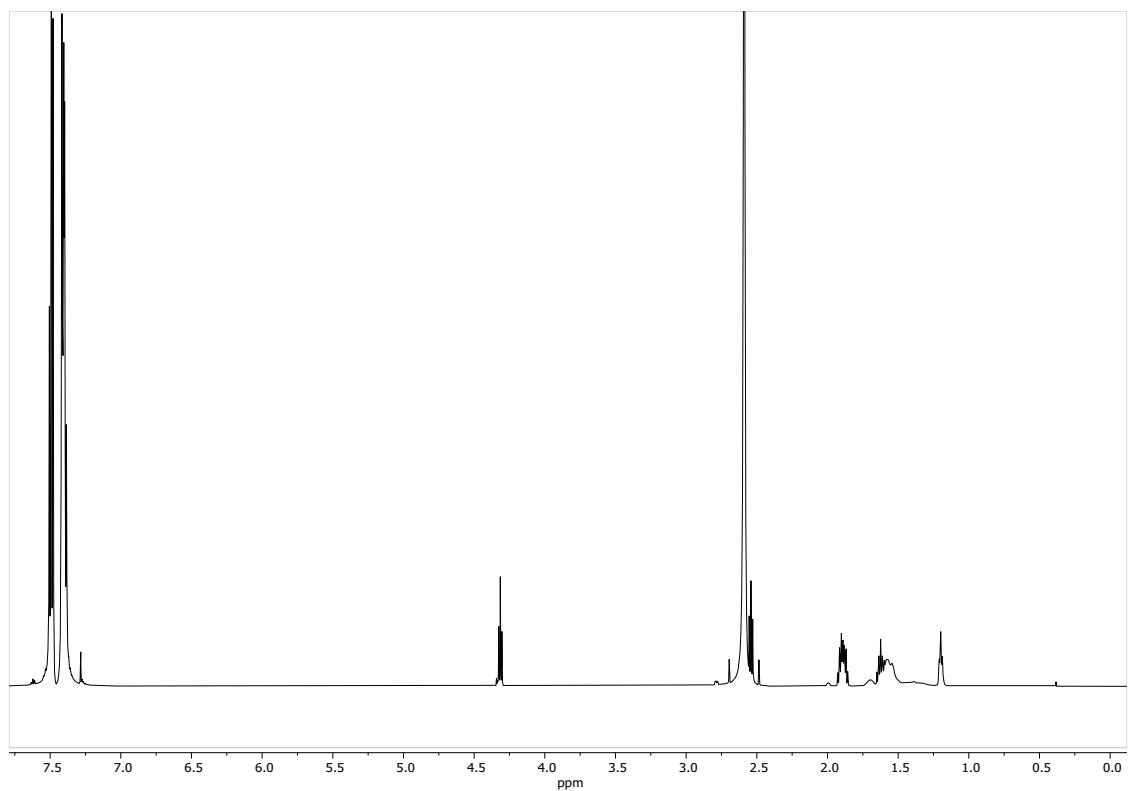


Figure S8: Representative crude ^1H NMR spectrum of a typical 1-hexene/ ϵ -CL copolymerisation using catalyst **1**/ $\text{BnB}(\text{C}_6\text{F}_5)_3^-$ in toluene, analysed in CDCl_3 at 20°C .

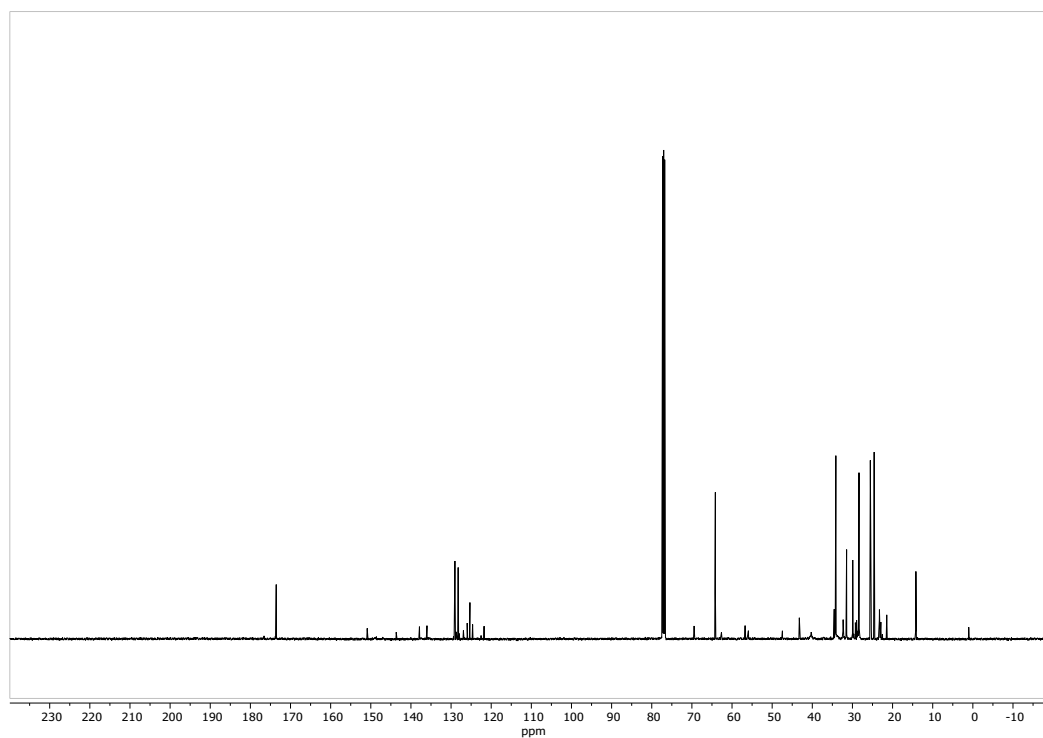


Figure S9: Crude ^{13}C NMR spectrum of a 1-hexene (10 equiv.)/ ϵ -CL (10 equiv) copolymerisation mixture using catalyst **1**/ $\text{BnB}(\text{C}_6\text{F}_5)_3^-$ in toluene, analysed in CDCl_3 at 20°C . The lack of resonances in the ketone region indicated the absence of junction units between PH and PCL polymers.

MALDI-ToF spectra of obtained polymers

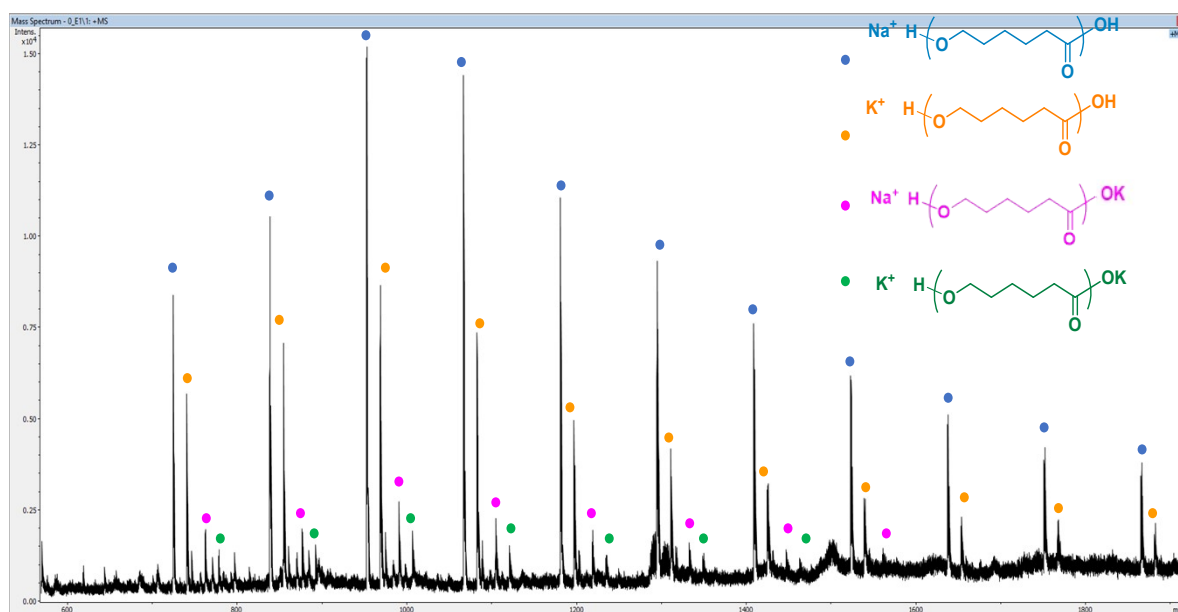


Figure S10: MALDI-ToF spectrum of PCL generated from the homopolymerisation of CL using $1/\text{BnB}(\text{C}_6\text{F}_5)_3^-$.

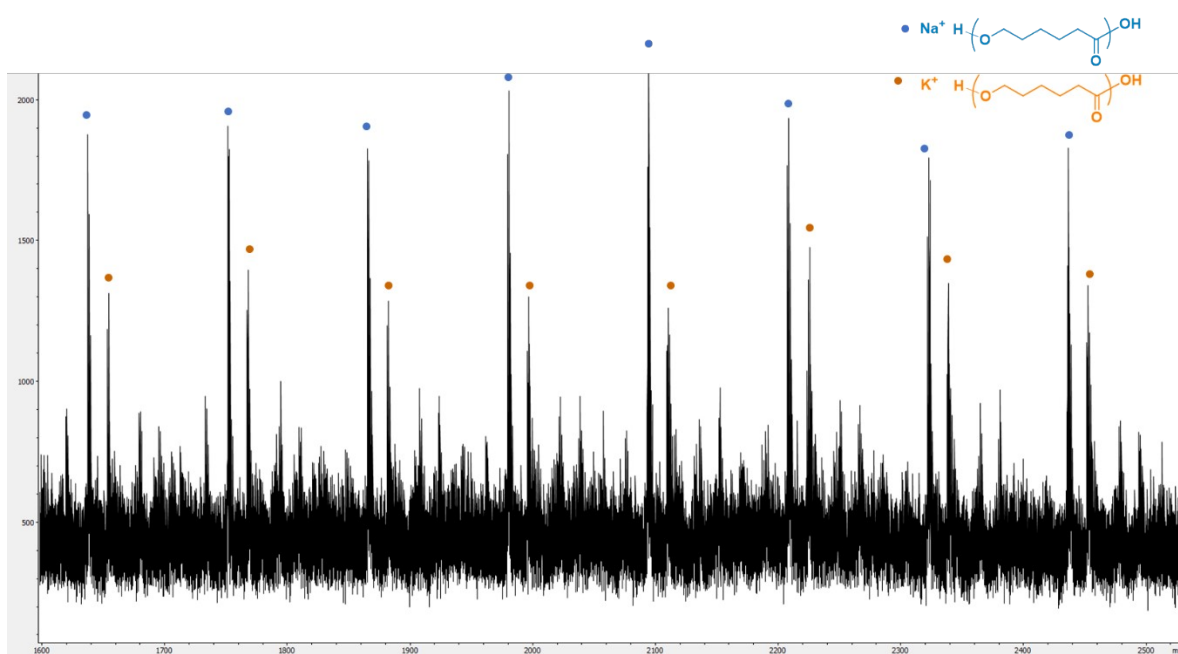


Figure S11: MALDI-ToF spectrum of PCL generated by the sequential addition of CL after 1-hexene polymerisation, using $1/\text{BnB}(\text{C}_6\text{F}_5)_3^-$ catalyst.

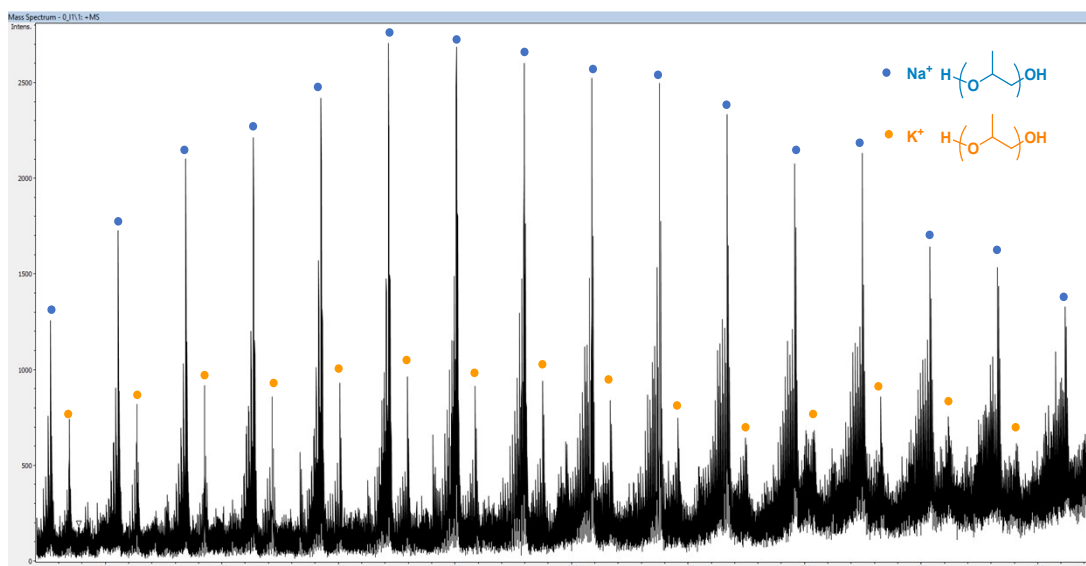


Figure S12: MALDI-ToF spectrum of PPO generated by the sequential addition of PO after 1-hexene polymerisation using $1/\text{BnB}(\text{C}_6\text{F}_5)_3^-$ catalyst.

SEC chromatograms of obtained polymers

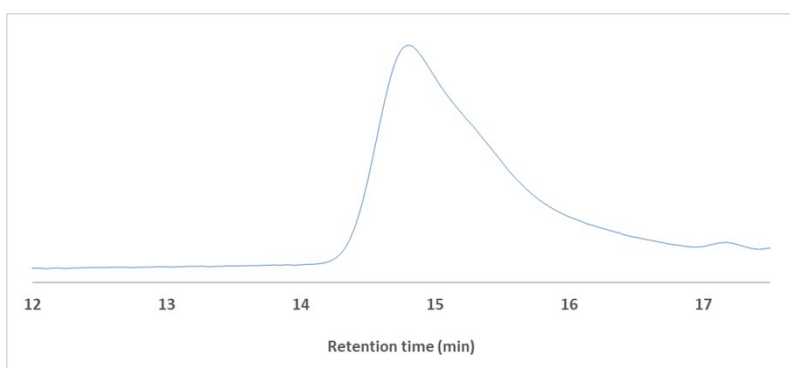


Figure S13: Typical SEC chromatogram of polyhexene produced using catalyst $1/\text{BnB}(\text{C}_6\text{F}_5)_3^-$.

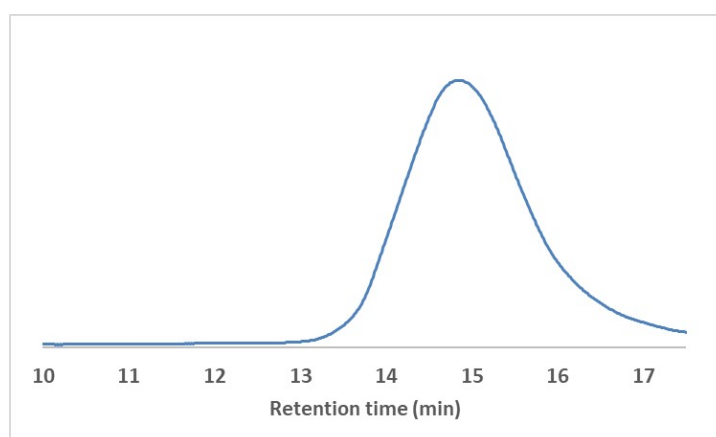


Figure S14: Typical SEC chromatogram of PCL produced using catalyst $1/\text{BnB}(\text{C}_6\text{F}_5)_3^-$.

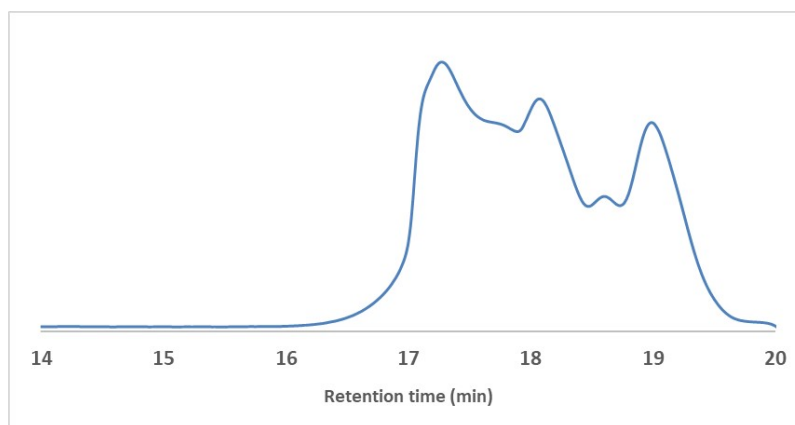


Figure S15: Typical SEC chromatogram of a PPO oligomers produced using catalyst $1/BnB(C_6F_5)_3^-$.

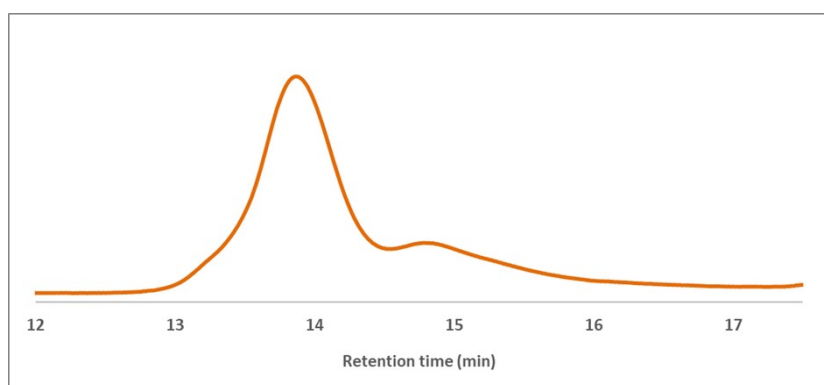


Figure S16: Typical SEC chromatogram of polymers produced *via* the sequential polymerisation of 1-hexene and CL using catalyst $1/BnB(C_6F_5)_3^-$.

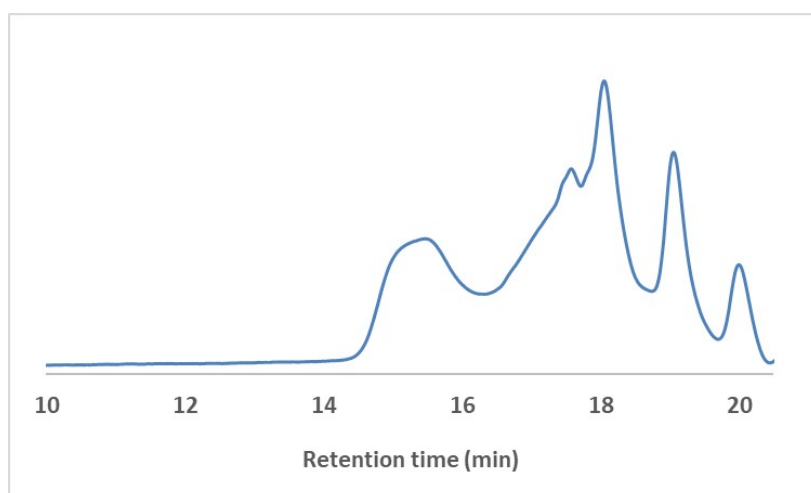


Figure S17: Typical SEC chromatogram of polymers/oligomers produced *via* sequential polymerisation of 1-hexene and PO using catalyst $1/BnB(C_6F_5)_3^-$.

DFT calculations

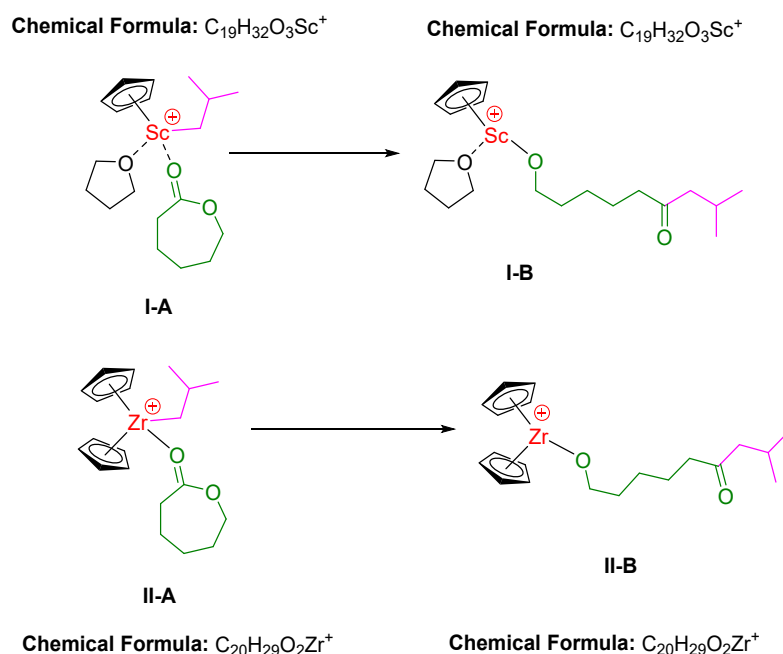


Figure S18: Structures of Sc and Zr metallocene catalysts bearing an isobutyl moiety (representing the PH chain) and the insertion of 1 equivalent of CL.

Table S2: Optimisation energies (U = internal, G = free energy) for **I-A**, **I-B**, **II-A**, **II-B**, calculated at M06/6-311G*/lan12dz level.

Compound	U/ M06/lan12dz /Hartrees	ΔU /kJmol ⁻¹	G/ M06/lan12dz /Hartrees	ΔG /kJmol ⁻¹
I-A	-1014.50498420	0	-1014.080136	0
I-B	-1014.82741357	-846.5	-1014.415886	-881.5
II-A	-975.662823260	0	-975.269510	0
II-B (1 imag. freq.)	-975.958141454	-775.3	-975.575480	-803.3

Table S3: Local force constants for **I-A**, **I-B**, **II-A** and **II-B**, calculated at the M06/6-311G*/lan12dz level.

	M=Sc		M=Zr	
	Distance/Å	Local force constant/ mDynÅ ⁻¹	Distance/Å	Local force constant/ mDynÅ ⁻¹
Compounds I-A + II-A				
M–O(lactone)	2.133	1.245	2.206	1.278
M–C(isobutyl)	2.162	1.643	2.288	1.509
M–Cp	2.42-2.45	0.89-0.84	2.48-2.53	1.13-1.00
M–O(THF)	2.168	1.200	–	–
Av. C–C lactone	1.49-1.52	4.3-4.2		
Compounds I-B + II-B				
M–O	1.832	4.33	1.927	3.914
M–Cp	2.40-2.44	1.07-0.91	2.48-2.52	1.0-0.99
M–O(THF)	2.131	1.469	–	–

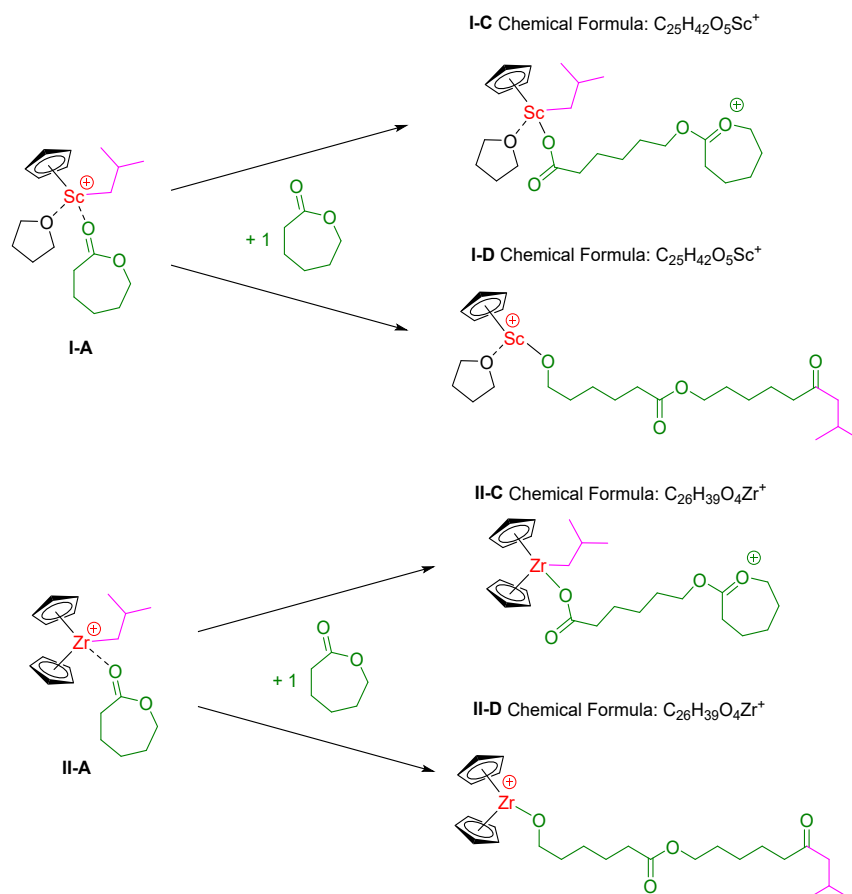


Figure S19: Structures of Sc and Zr metallocene catalysts bearing an isobutyl moiety (representing the PH chain) and the insertion of 2 equivalents of CL.

Table S4: Optimisation energies (U = internal, G = free energy) for I-A/C/D and II-A/C/D, and lactone (CL), calculated at M06/lanl2dz level.

Compound	U/ M06/lanl2dz /Hartrees	G/ M06/lanl2dz /Hartrees
I-A	-1014.50498420	-1014.080136
II-A	-975.663823260	-975.2699510
lactone	-384.803541131	-384.678398
I-C	-1399.28723476	-1398.724013
I-D	-1399.33705694	-1398.779094
II-C	-1360.45191162	-1359.919711
II-D	-1360.46991319	-1359.943856

Table S5: Free energies for chemical pathways, calculated at M06/lanl2dz level

Pathway	Reactants /Hartrees	Products /Hartrees	$\Delta G(\text{Products-reactants})$ /Hartrees	$\Delta G(\text{Products-reactants})$ /kJmol ⁻¹
I-A → I-C	-1398.758534	-1398.724013	+0.034521	+90.6
I-A → I-D	-1398.758534	-1398.779094	-0.02056	-54.0
II-A → II-C	-1359.948349	-1359.919711	+0.028638	+75.2
II-A → II-D	-1359.948349	-1359.943856	+0.004493	+11.8

Computational methods: Calculations for all compounds were performed at M06/(Sc, Zr: lanl2dz, first row elements: D95V) M06/(Sc, Zr: lanl2dz, first row elements: 6-311G*) level using Gaussian16.⁹ Input files were constructed using Z-matrix notation, and all optimised structures obtained were confirmed as minima through the calculation of 3N-6 real vibrational frequencies, with the exception of II-B for which one low-lying imaginary frequency (at -7 cm⁻¹) remained. Animation of the eigenvector indicated that this corresponded to the conformation of the long polymer chain. Given the high degree of flexibility in this part of the structure this outcome was not unexpected. Local force constants, which are mass-independent measures of bond strengths, were calculated from the normal mode force constant matrices using LMODEA.¹⁰

References

1. E. Y. Tshuva, I. Goldberg and M. Kol, *J. Am. Chem. Soc.*, 2000, **122**, 10706-10707.
2. E. Y. Tshuva, M. Versano, I. Goldberg, M. Kol, H. Weitman and Z. Goldschmidt, *Inorg. Chem. Commun.*, 1999, **2**, 371-373.
3. S. C. Kosloski-Oh, Y. Manjarrez, T. J. Boghossian and M. E. Fieser, *Chem. Sci.*, 2022, **13**, 9515-9524.
4. E. Fazekas, G. S. Nichol, J. A. Garden and M. P. Shaver, *ACS Omega*, 2018, **3**, 16945-16953.
5. T. Sârbu and E. J. Beckman, *Macromolecules*, 1999, **32**, 6904-6912.
6. V. Sessini, M. Palenzuela, J. Damián and M. E. G. Mosquera, *Polymer*, 2020, **210**, 123003.
7. J. Bruckmoser, S. Pongratz, L. Stieglitz and B. Rieger, *J. Am. Chem. Soc.*, 2023, **145**, 11494-11498.
8. W. Gruszka and J. A. Garden, *Chem. Commun.*, 2022, **58**, 1609-1612.
9. M. J. Frisch, G. W. Trucks, H. B. Schlegel, G. E. Scuseria, M. A. Robb, J. R. Cheeseman, G. Scalmani, V. Barone, G. A. Petersson, H. Nakatsuji, X. Li, M. Caricato, A. V. Marenich, J. Bloino, B. G. Janesko, R. Gomperts, B. Mennucci, H. P. Hratchian, J. V. Ortiz, A. F. Izmaylov, J. L. Sonnenberg, Williams, F. Ding, F. Lipparini, F. Egidi, J. Goings, B. Peng, A. Petrone, T. Henderson, D. Ranasinghe, V. G. Zakrzewski, J. Gao, N. Rega, G. Zheng, W. Liang, M. Hada, M. Ehara, K. Toyota, R. Fukuda, J. Hasegawa, M. Ishida, T. Nakajima, Y. Honda, O. Kitao, H. Nakai, T. Vreven, K. Throssell, J. A. Montgomery Jr., J. E. Peralta, F. Ogliaro, M. J. Bearpark, J. J. Heyd, E. N. Brothers, K. N. Kudin, V. N. Staroverov, T. A. Keith, R. Kobayashi, J. Normand, K. Raghavachari, A. P. Rendell, J. C. Burant, S. S. Iyengar, J. Tomasi, M. Cossi, J. M. Millam, M. Klene, C. Adamo, R. Cammi, J. W. Ochterski, R. L. Martin, K. Morokuma, O. Farkas, J. B. Foresman and D. J. Fox, Wallingford, CT, 2016.
10. E. Kraka, M. Quintano, H. W. La Force, J. J. Antonio and M. Freindorf, *J. Phys. Chem. A*, 2022, **126**, 8781-8798.